BOUNDARY-LAYER CIRCULATION IN TURBULENT ROTATING CONVECTION

Rudie Kunnen*, Richard Stevens**, Jim Overkamp*, Chao Sun**, GertJan van Heijst* & Herman Clercx*[a)]
*Department of Applied Physics and J.M. Burgers Centre for Fluid Dynamics, Eindhoven University of Technology, P.O. Box 513, 5600 MB Eindhoven, The Netherlands
**Department of Science and Technology and J.M. Burgers Centre for Fluid Dynamics, University of Twente, P.O. Box 217, 7500 AE Enschede, The Netherlands

Summary Rotation adds interesting dynamics to buoyancy-driven turbulence. In this work a volume of water in an upright cylinder closed from above with a cooled plate and from below with a heated plate is rotated about the cylinder axis. A transition of the dominant flow structure from a single roll to an ensemble of vortical columns is reflected in the convective heat transfer, which increases under certain rotation rates. The vortices are connected to Ekman boundary layers on the plates which directly affect the bulk flow and drive a secondary circulation. We study this boundary-layer-driven recirculation with numerical simulation and interpret temperature measurements from the sidewall of a rotating-convection experiment.

ROTATING RAYLEIGH-BÉNARD CONVECTION

The classical system to study buoyancy driven flows is the Rayleigh-Bénard (RB) system (see the recent reviews in Refs. [1, 2] for an overview). In this system a layer of fluid is confined between two horizontal plates and is heated from below and cooled from above. The RB system is also very suitable to study the influence of rotation on heat transport mechanisms. In order to do this the RB system is rotated at an angular speed Ω about its vertical axis. Studies about the influence of rotation on heat transport are relevant to understand many geophysical and astrophysical flow phenomena such as the global thermohaline circulation, convection in the interior of gaseous planets, and convection in the outer layer of the Sun. Furthermore, the studies are also very relevant for optimization of industrial applications.

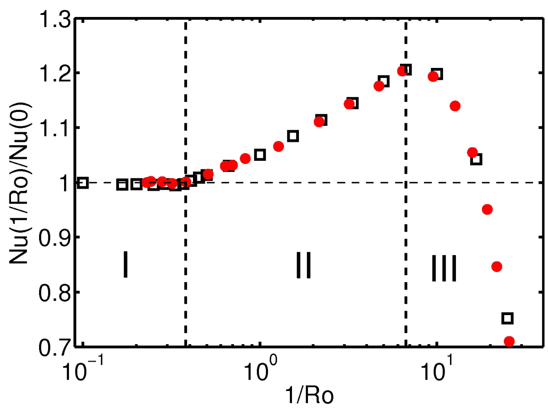

Figure 1. The scaled heat transfer $Nu(1/Ro)/Nu(0)$, with Nu the Nusselt number defined in the text, as function of $1/Ro$ on a logarithmic scale. Experimental and DNS data for $Ra = 2.73 \times 10^8$ and $Pr = 6.26$ are indicated by red dots and open squares, respectively (from Refs. [3] and [4]). The transition between the different regimes is indicated by the vertical dashed lines.

The rotation rate around the vertical axis is indicated by the Rossby number Ro, which compares the inertial and Coriolis forces in the system. Here, Ro is defined as $Ro = \sqrt{Ra/(PrTa)}$, where $Pr = \nu/\kappa$ is the Prandtl number, $Ta = (2\Omega L^2/\nu)^2$ is the Taylor number and $Ra = \beta g L^3 \Delta/(\nu\kappa)$ is the Rayleigh number, with Ω the rotation rate, β the thermal expansion coefficient, g the gravitational acceleration, ν the kinematic viscosity, κ the thermal diffusion coefficient, and Δ the temperature difference between the two plates. We will consider a cell with aspect ratio $\Gamma = D/L = 1$, with L the height of the RB cell and D its diameter. The dimensionless heat transport in the system is indicated by the Nusselt number, $Nu = QL/(\lambda\Delta)$, where Q is the heat-current density and λ is the thermal conductivity of the fluid in the absence of convection.

Three distinct regimes

In figure 1 we show a typical measurement of the heat transport enhancement with respect to the non-rotating case as function of the rotation rate [3, 4]. The figure shows that, depending on the rotation rate, three different regimes can be identified. Regime I (weak rotation), where no heat transport enhancement is observed, regime II (moderate rotation), where a strong heat transport enhancement is found, and regime III (strong rotation), where the heat transport starts to decrease. Flow visualization experiments and analysis of the flow structures obtained in numerical simulations have confirmed that this division of regimes coincides with changes observed in flow patterns and flow characteristics [5, 4, 6].

a) Corresponding author. E-mail: h.j.h.clercx@tue.nl.

In regime I ($1/Ro \lesssim 0.5$) the large scale circulation (LSC), typical for non-rotating RB convection, is still present, because the Coriolis force is too weak to overcome the buoyancy force that causes the LSC. In Ref. [4] it was shown that there is a sharp transition to the regime where rotational effects become important, while at the same time the strength of the LSC is decreasing [7]. In regime II ($0.5 \lesssim 1/Ro \lesssim 6.7$) the LSC is replaced by predominantly vertically oriented vortical columns as the dominant flow structures and a large increase in the heat transport is observed. This enhanced heat transport has been ascribed to Ekman pumping ([8, 9, 10, 7, 11, 4]). The effect of Ekman pumping, and thus the observed heat transfer enhancement, depends strongly on the $Ra-$ and $Pr-$ values, see Refs. [3, 12]. When the rotation rate is increased further a large decrease in the heat transport is observed, because the vertical velocity fluctuations are suppressed due to the rotation [13, 6]. We will call this regime III.

The role of Stewartson and Ekman layers in rotating Rayleigh-Bénard convection

In this contribution we address the question of how these different regimes can be identified from measurements of the azimuthal wall temperature distribution and the vertical temperature gradient along the sidewall, with probes that are embedded in the sidewall of a RB convection cell. The azimuthal temperature profiles at the sidewall as function of the rotation rate is obtained from experiments and compared with the azimuthal temperature and vertical velocity profiles close to the sidewall found in direct numerical simulations (DNS). In order to explain the sidewall temperature measurements we have studied the azimuthally averaged flow profiles obtained from DNS (see figure 2). The analysis shows that the sidewall temperature measurements, particularly the presence of the vertical wall temperature gradients in regimes II and III, can be explained by the presence of Stewartson layers that are formed along the sidewall [14].

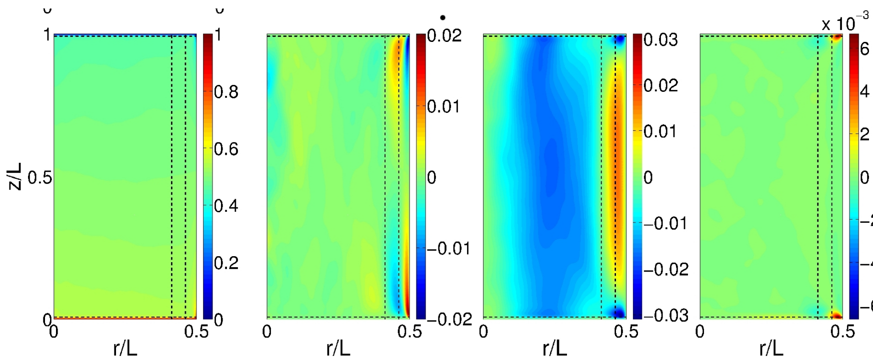

Figure 2. The figures from left to right indicate the temporal and azimuthal averages of temperature and the velocity components u_z, u_ϕ, and u_r, respectively, for $Ra = 1.00 \times 10^9$, $Pr = 6.4$, and $1/Ro = 2.78$ (regime II). The left-hand side of each picture is the cylinder axis $r = 0$; the right-hand side corresponds to the sidewall $r/L = 0.5$. The dashed lines indicate typical Ekman boundary-layer thicknesses near the bottom and top plates, and Stewartson boundary-layer thicknesses near the sidewall from linear boundary-layer theory.

References

[1] Ahlers G., Grossmann S., Lohse D.: Heat transfer and large scale dynamics in turbulent Rayleigh-Bénard convection. *Rev. Mod. Phys.* **81**, 503, 2009.

[2] Lohse D., Xia K. Q.: Small-scale properties of turbulent Rayleigh-Bénard convection. *Annu. Rev. Fluid Mech.* **42**, 335–364, 2010.

[3] Zhong J.-Q., Stevens R.J.A.M., Clercx H.J.H., Verzicco R., Lohse D., Ahlers G.: Prandtl-, Rayleigh-, and Rossby-number dependence of heat transport in turbulent rotating Rayleigh-Bénard convection. *Phys. Rev. Lett.* **102**, 044502, 2009.

[4] Stevens R.J.A.M., Zhong J.-Q., Clercx H.J.H., Ahlers G., Lohse, D.: Transitions between turbulent states in rotating Rayleigh-Bénard convection. *Phys. Rev. Lett.* **103**, 024503, 2009.

[5] Boubnov B.M., Golitsyn G.S.: Temperature and velocity field regimes of convective motions in a rotating plane fluid layer. *J. Fluid Mech.* **219**, 215–239, 1990.

[6] Kunnen R.P.J., Geurts B.J., Clercx H.J.H.: Experimental and numerical investigation of turbulent convection in a rotating cylinder. *J. Fluid Mech.* **642**, 445–476, 2010.

[7] Kunnen R.P.J., Clercx H.J.H., Geurts, B.J.: Breakdown of large-scale circulation in turbulent rotating convection. *Europhys. Lett.* **84**, 24001, 2008.

[8] Rossby H.T.: A study of Bénard convection with and without rotation. *J. Fluid Mech.* **36**, 309–335, 1969.

[9] Julien K., Legg S., McWilliams J., Werne J. Hard turbulence in rotating Rayleigh–Bénard convection. *Phys. Rev. E* **53**, R5557–R5560, 1996.

[10] Vorobieff P., Ecke R.E.: Turbulent rotating convection: an experimental study. *J. Fluid Mech.* **458**, 191–218, 2002.

[11] King E.M., Stellmach S., Noir J., Hansen U., Aurnou J.M.: Boundary layer control of rotating convection systems. *Nature* **457**, 301, 2009.

[12] Stevens R.J.A.M., Clercx H.J.H., Lohse D.: Optimal Prandtl number for heat transfer in rotating Rayleigh-Bénard convection. *New J. Phys.* **12**, 075005, 2010.

[13] Kunnen R.P.J., Clercx H.J.H., Geurts B.J.: Enhanced vertical inhomogeneity in turbulent rotating convection. *Phys. Rev. Lett.* **101**, 174501, 2008.

[14] Kunnen R.P.J., Stevens R.J.A.M., Overkamp J., Sun C., van Heijst G.J.F., Clercx H.J.H.: The role of Stewartson and Ekman layers in turbulent rotating Rayleigh-Bénard convection. *J. Fluid Mech.* **688**, 422–442, 2011.